

STNet: Scale Tree Network with Multi-level Auxiliator for Crowd Counting

Mingjie Wang^{1,2}, Hao Cai², Xianfeng Han³, Jun Zhou⁴, Minglun Gong^{1*}

¹University of Guelph, ON, Canada

²Memorial University of Newfoundland, NL, Canada

³Southwest University, Chongqing, China

⁴Dalian Maritime University, Dalian, China

Abstract

Crowd counting remains a challenging task because the presence of drastic scale variation, density inconsistency, and complex background can seriously degrade the counting accuracy. To battle the ingrained issue of accuracy degradation, we propose a novel and powerful network called Scale Tree Network (STNet) for accurate crowd counting. STNet consists of two key components: a Scale-Tree Diversity Enhancer and a Semi-supervised Multi-level Auxiliator. Specifically, the Diversity Enhancer is designed to enrich scale diversity, which alleviates limitations of existing methods caused by insufficient level of scales. A novel tree structure is adopted to hierarchically parse coarse-to-fine crowd regions. Furthermore, a simple yet effective Multi-level Auxiliator is presented to aid in exploiting generalisable shared characteristics at multiple levels, allowing more accurate pixel-wise background cognition. The overall STNet is trained in an end-to-end manner, without the needs for manually tuning loss weights between the main and the auxiliary tasks. Extensive experiments on four challenging crowd datasets demonstrate the superiority of the proposed method.

Introduction

Crowd counting recently has drawn lots of attention from researchers due to its great importance in a wide array of real-world applications including video surveillance, public crowd monitoring, and traffic control. The main objective of crowd counting is to infer the number of people in congested images (Jiang et al. 2020a). Despite the exploration of pioneer works (Zhang et al. 2016; Sam, Surya, and Babu 2017; Cao et al. 2018; Li, Zhang, and Chen 2018; Liu, Salzmann, and Fua 2019; Jiang et al. 2020a), crowd understanding is still a challenging issue for scenes exhibiting drastic scale variations, density inconsistency, or complex background.

Along with the growing learning ability of deep neural networks, dozens of CNN-based solutions are sprung to tackle the aforementioned nuisances. The issue of scale variations (see Figure 1) has attracted considerable attention from the research community (Zhang et al. 2016; Sam, Surya, and Babu 2017; Sindagi and Patel 2017; Cao et al. 2018; Liu et al. 2019a; Sindagi and Patel 2019; Liu, Yang, and Ding 2020; Bai et al. 2020; Jiang et al. 2020a). These methods endeavour to exploit multi-scale features through fusing representations from multiple layers (Sindagi and Patel 2019), branches (Bai et al. 2020) or columns (Zhang et al.

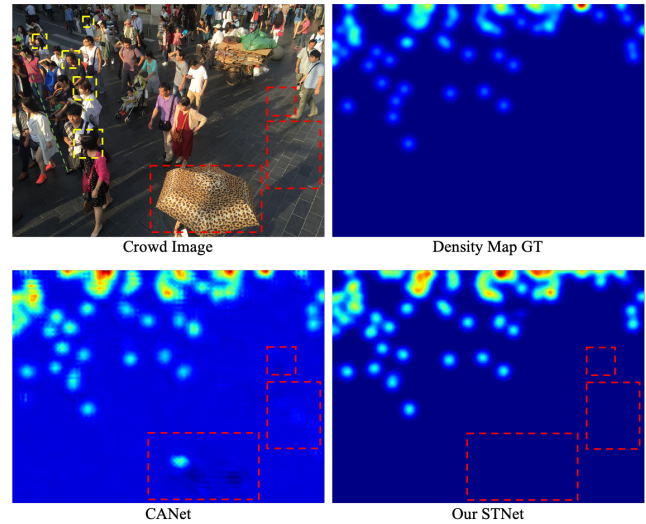


Figure 1: Scale variations (yellow boxes) and complex background noises (red boxes) can often confuse existing approaches, such as CANet (Liu, Salzmann, and Fua 2019). In comparison, our approach properly handles these areas.

2016; Sam, Surya, and Babu 2017) with varied receptive field sizes. However, all these methods only mine a limited range of scales in a coarse manner and hence do not perform well under wide scale diversity and uncertainty of scale variations. Accordingly, an adequate scale diversity is desired to conform with the rapid intra- and inter-image scale changes of crowd heads or background objects.

In fact, the procedure of scale parsing tends to be hierarchically structured (coarse-to-fine): smaller units (e.g., small heads) are nested within larger units (e.g., foreground region) (Shen et al. 2019), which are overlooked by most of existing methods. S-DCNet (Xiong et al. 2019) attempts to utilize the spatial divide-and-conquer to decompose the counting. However, splitting the feature map into four sub-regions with the same area destroys the holistic geometric and semantic attributes of representations. The underlying structure for hierarchically parsing crowd has not been fully investigated in terms of fine-grained scale decomposition. Inspired by the promising application of tree structure in

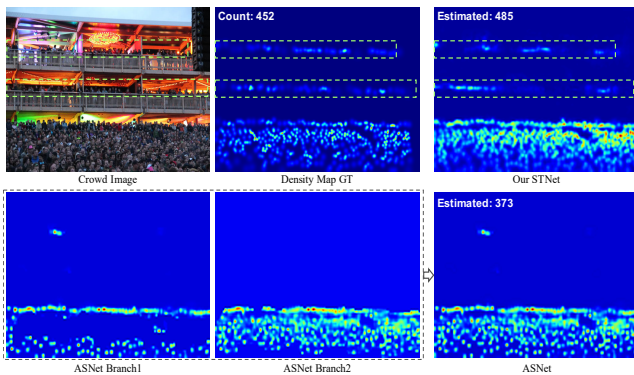


Figure 2: Bounded by limited and discrete density levels, ASNet (Jiang et al. 2020a) fails to generate an accurate density map (bottom row) for the input scene from ShanghaiTech Part_A (Zhang et al. 2016). In comparison, the density map and counting result of our approach are much closer to the ground truth.

NLP (Shen et al. 2019), we creatively integrate it to counting network for coarse-to-fine scale modeling, as well as for explicit expansion of scale range.

Density change across crowd scenes is also an open issue that causes accuracy degradation. While existing approaches (Liu, Salzmann, and Fua 2019; Xiong et al. 2019; Sindagi and Patel 2019; Jiang et al. 2020a) have tried to address this by re-weighting multiple branches with different density distributions, such approaches are prone to under- or over-fitting due to manually-designed levels and inconsistency of different branches. As shown in Figure 2, even though two scale branches are utilized, ASNet (Jiang et al. 2020a) still cannot capture accurate people distributions in this example. The essence of these methods is to boost multiple columns to independently encode regions with different people densities. To alleviate the limitations of multi-branch-based methods, it is desired to impel a single-column network to gather hints that can accommodate density shifts.

As shown in Figure 1, complex background is another factor that should not be neglected for accurate counting. Objects presenting in the background can vary dramatically (floor, umbrella, shadow, tree, etc.). Hence, precise background filtering is vital to relieve pressure of density prediction. Considering the density-map-based paradigm, ground truth of density map is generated by convolving annotation map to indicate density values which are entangled with weak location information at each pixel. Therefore, the supervision of density map inevitably propagates the inherent ambiguity of signals, compounded by inconsistent numerical and semantic distributions, into learning procedure, which in turn negatively affects background filtering in the case of limited training set (Gao et al. 2017). Even though the SDANet (Miao et al. 2020) is empowered by focusing more on regions being crowd, the attention mechanism is optimized along with the main backbone through minimizing the L_2 error of density maps, which ignores the ambiguity problem. Another promising line of explorations (Liu et al.

2019b; Zhao et al. 2019; Jiang et al. 2020a) is to leverage auxiliary tasks (e.g., classification) to aid in the density estimation. It is observed that these methods bring minor benefits for extracting density- and background-aware characteristics. The deficiencies mainly arise from following reasons:

- Overlooking features from different levels impedes the encoding of fine-grained crowd regions. It is well-known that features from low-level layers encode details and spatial information, which can be exploited to achieve better localization (Miao et al. 2020). Meanwhile, high-level representations encode global context (Zhao et al. 2019; Sindagi and Patel 2019) with multi-scale information.
- The insufficient relationship of knowledge from auxiliary stages (e.g. classification, segmentation, counting number and density estimation) causes the phenomenon that optimization directions of auxiliary branches are not conformable with each other (Li and Chen 2020).
- There is a serious frequency imbalance of crowd and background pixels. For example, the percentage of background pixels is only 0.1867 in Part_A and this observation is also supported by S-DCNet (Xiong et al. 2019). The imbalance results in failing to capture discriminative features for the cognition of complex background.
- Finally, the training proceeds in a multi-stage manner and loss weights are manually tuned, which is tedious and prone to bias among side tasks. It is vital for multi-task learning to mine generalisable features. Loss supervisions should also enable learning of all tasks with equal contribution without allowing some tasks (e.g. density estimation) to dominate (Liu, Johns, and Davison 2019).

Towards the aforementioned issues, in this paper we coherently tackle wide-range scale variations, density inconsistency, and highly complex backgrounds for further performance improvement. To this end, we propose a novel *Scale Tree Network* (STNet), see Figure 3, which is end-to-end trainable. Instead of simply stacking parallel branches at multiple scales, we delicately design a parameter-efficient *Scale Tree Diversity Enhancer* to widen the range of receptive fields and achieve the hierarchical parsing of coarse-to-fine scales.

Furthermore, inspired by the success of multi-task learning (Sindagi and Patel 2017; Zhao et al. 2019), we reformulate the problems of density shift and complex background as a single *multi-level confidence-driven attribute* instead of superfluous attributes which are unconformable with each other and heavily rely on manually specified density classification. This new form of attribute disentangles localization/global density distribution information inheriting from original density map. It also helps impose collaborative hints for crowd estimation on multi-level shared layers. Hence, we present a simple yet effective *Semi-supervised Multi-level Auxiliator*, which aims at facilitating the shared characteristics of the backbone CNN to embed crowd localization, holistic density distribution along with scale information.

Apart from novelty on network architecture, our approach also differs in training procedure. Specifically, all of our proposed components are optimized jointly in an end-to-

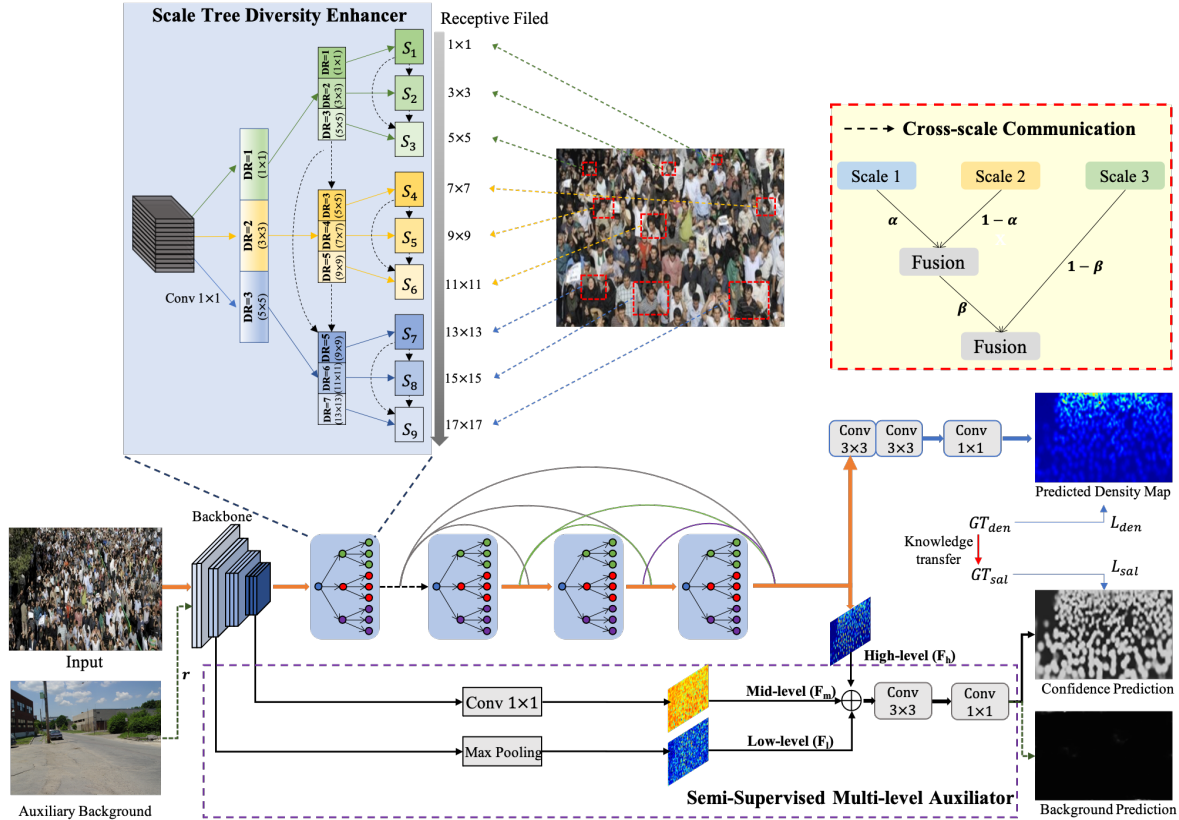


Figure 3: Architecture overview of the proposed STNet. The network consists of two key components: Scale Tree Diversity Enhancer and Semi-supervised Multi-level Auxiliator. α and β in cross-scale communication are random weights obeying the uniform distribution between 0 and 1. r indicates the percentage of pure background images for semi-supervision and DR in the enhancer denotes the dilation rate. The whole network is trained in an end-to-end fashion.

end manner. As shown in Figure 1, the intrinsically cluttered background is usually mistakenly regarded as crowd due to the imbalance of background and crowd pixels, particularly in dataset with highly congested scenes. To address this issue, a semi-supervision strategy is incorporated when optimizing the auxiliary task through utilizing a number of unlabelled and pure background images. Extensive experiments conducted on four popular crowd benchmarks (ShanghaiTech Part A and Part B (Zhang et al. 2016), UCF_QNRF (Idrees et al. 2018), UCF_CC_50 (Idrees et al. 2013)) demonstrate the superiority of our proposed method over state-of-the-art with best or competitive accuracy.

Related Work

Recent years have witnessed the progress of crowd counting. The early approaches (Zhao and Nevatia 2003; Sidla et al. 2006; Li et al. 2008; Subburaman, Descamps, and Carincotte 2012) formulate the counting issue as a detection problem, which utilizes the hand-crafted low-level features to detect human parts. These approaches usually deliver poor results in congested images due to severe occlusion. Thus, density regression has been widely utilized to improve the counting accuracy, which maps features to density map (Chan, Liang,

and Vasconcelos 2008; Chen et al. 2013, 2012; Lempitsky and Zisserman 2010; Pham et al. 2015). Then the overall count is calculated by summing values over the predicted density map. Thanks to the power of deep learning, CNN-based methods have become the mainstream of crowd analysis. We here review them based on their design objectives.

To handle scale variations. This group of approaches aim at mining multi-scale representations to address huge scale changes. MCNN (Zhang et al. 2016) leverages multiple columns to obtain features of multi-size receptive fields. Hydra-CNN (Onoro-Rubio and López-Sastre 2016) learns a multi-scale non-linear regressor using a pyramid of input patches. Switch-CNN (Sam, Surya, and Babu 2017) incorporates a side classifier to assign crowd patch to the appropriate estimation sub-model. Sindagi *et al.* (Sindagi and Patel 2017) propose to combine global and local contextual information for multi-scale features extraction. CSRNet (Li, Zhang, and Chen 2018) and ADCrowdNet (Liu et al. 2019b) prove the effectiveness of dilated and deformable convolutions on expanding receptive fields. Recently, CAN (Liu, Salzmann, and Fua 2019) adaptively encodes the scale of the contextual information. MBTTBF (Sindagi and Patel 2019) employs a principled way of generating scale-aware super-

vision for training to increase the effectiveness of scale integration. DSSINet (Liu et al. 2019a) employs CRFs to refine scale information with a message passing mechanism. Bai *et al.* (Bai et al. 2020) propose adaptive dilated convolution to adapt the scale variation. These approaches only consider limited scale diversity and discard the inherent hierarchical structure of parsing scale, which limits their ability to handle huge scale variations.

To tackle changes of density distribution. The common way to cope with density shifts is to learn rich representations covering adequate density levels. S-DCNet (Xiong et al. 2019) utilizes spatial divide-and-conquer strategy to recursively divide the dense scene into sub-regions with sparse crowd. Jiang *et al.* propose to use masks focusing on regions with different density levels to generate multi-branch density maps. DensityCNN (Jiang et al. 2020b) jointly trains a density-level classifier to provide guidance. However, manually tuning the number of density levels is notorious.

To mitigate the effects of background noises. Filtering noises (e.g. background pixels) in highly congested scenes has drawn growing attention from the community. One way to address this issue is to empower the network with attention mechanism for alleviating cluttered noises. Miao *et al.* (Miao et al. 2020) try to diminish the impact of backgrounds via involving a shallow feature-based attention module. Another way is to employ auxiliary tasks. AD-CrowdNet (Liu et al. 2019b) views this issue as a classification task and trains an additional attention-aware network to detect crowd regions, whereas Zhao *et al.* (Zhao et al. 2019) formulate it as segment attribute attached on intermediate layers to guide the backbone to gain representations with latent semantic information. However, there is still much room for improvement in driving the backbone to capture more robust features in a multi-level fashion.

Methodology

Scale Tree Diversity Enhancer

With the drive to handle the challenges of polytropic head scales, a series of methods have been raised to acquire multi-scale features by resorting to multi-layer/branch/column aggregation with limited scale diversity. To further amplify the number of scales that a single output layer can represent and hierarchically parse coarse-to-fine scale information, we propose a delicately designed Scale Tree Diversity Enhancer. The Diversity Enhancer recursively divides the filter channels into small filter groups indicating diverse receptive filed sizes. These filter groups are organized in a tree structure, which allows reusing computation results and hence minimizes computational overhead.

The pipeline of the proposed enhancer is shown in Figure 3. Following previous work (Li, Zhang, and Chen 2018), we adopt the first ten layers of pre-trained VGG-16 (Simonyan and Zisserman 2014) as the backbone to capture the low- and middle-level features. We then sequentially stack six scale tree diversity enhancers with dense connection for higher-level scale parsing. As demonstrated in Figure 4, unlike most existing approaches that process scale information by a layer-wise way, our enhancer proceeds in multi-scale

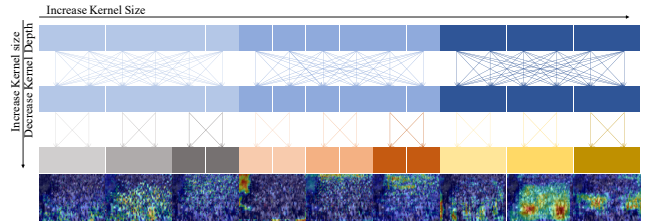


Figure 4: The details of scale tree in our model. The channels are split recursively and the number of groups ranges from 1, 3 to 9.

representations at a more granular level, which is based on group convolutions with kernel depths (number of input feature maps) and kernel sizes varying along two dimensions of channel and level. The Diversity Enhancer first compresses the channel of input feature (x) via 1×1 convolution T_0 and the output is viewed as the root of scale tree (parent scale F_0). Afterwards, the root features are split into three groups as nodes (children scales F_1) and then propagated to atrous convolution transformation T_i with dilation rates i in $\{1, 2, 3\}$. Recurrently, the nodes of second layer in the tree are deeply refined through dividing them into fine-grained leaves, followed by diverse sub-groups of dilated convolutions T_j with dilation rates j in $\{1, 2, 3, 3, 4, 5, 5, 6, 7\}$. To avoid the jumping change of receptive filed sizes, here dilation rates 3 and 5 are used twice. The terminal leaves (terminal scales F_2) involving abundant multi-scale information are concatenated into the next layer. Hence, the parsing procedure of the enhancer can be defined as:

$$\begin{cases} F_0 = T_0(W_0, X), \\ F_{1,n} = T_i(W_i, F_{0,n}), n \in \{1, 2, 3\} \\ F_{2,m} = T_j(W_j, F_{1,m}), m \in \{1, 2, \dots, 9\}, \end{cases} \quad (1)$$

where W_0 indicates the trainable parameters of 1×1 convolution T_0 . W_i denotes the path weights in the tree from parent scale F_0 to children scales F_1 , whereas W_j corresponds to the path weights from children scales F_1 to terminal scales F_2 , respectively. The number of paths from root to leaves in our scale tree is used to characterize the scale diversity. In our implementation, the number of output scales is 9 and the maximum receptive filed size can reach to 17×17 .

Cross-scale Communication. Existing methods face the challenge of learning complementary scales on account of the ambiguity hiding in correlated adjacent scales (Sindagi and Patel 2019). To avoid this issue and break the co-adaptation among children nodes in the scale tree, we design a mechanism of stochastic cross-scale communication. As shown in Figure 3 (dotted box in red), the children scales S_1 , S_2 and S_3 with receptive field sizes ranging from small to large ($S_1 < S_2 < S_3$) deliver message through recursive refinement. We formulate the communication as:

$$\hat{S}_1 = S_1, \hat{S}_2 = \alpha \hat{S}_1 + (1 - \alpha) S_2, \hat{S}_3 = \beta \hat{S}_2 + (1 - \beta) S_3, \quad (2)$$

where α and β are random weights obeying the uniform distribution between 0 and 1. Before each training epoch, all variable gates are overwritten with new random values,

while they are set to expected value of 0.5 during inference. By doing this, complementary scales are deeply exploited thanks to the reduction of ambiguity among children scales by stochastically blocking. The additional advantage of cross-scale communication is to provide regularization cue for preventing overfitting.

Complexity Analysis. Albeit tree-like structure seems to be complex, our scale enhancer is lightweight due to ingenious organization of various dilated convolutions. The standard convolution usually contains a single type of kernel with kernel size K^2 and depth D . As for a standard computation block, it is comprised of one 1×1 conv layer and two layers of equal depths kernel size 3^2 and depth D . The number of parameters (P) and FLOPs can be computed as:

$$P = D^2 + 2 \times 9D^2 = 19D^2, FLOPs = 19D^2WH, \quad (3)$$

where W and H denote the spatial width and height of feature maps, respectively. Analogously, the number of parameters and FLOPs for our tree-based enhancer are:

$$P = D^2 + 3 \times 9\left(\frac{D}{3}\right)^2 + 9 \times 9\left(\frac{D}{9}\right)^2 = 5D^2 \quad (4)$$

$$FLOPs = 5D^2WH \quad (5)$$

With this formulation, our proposed module is more parameter-efficient ($5D^2 < 19D^2$) than multi-scale processing based on standard convolutions.

Semi-supervised Multi-level Auxiliator

Multi-level Auxiliator. To optimize for auxiliary tasks, previous approaches simply attach side supervisions to the top-most layer of feature extractor (Zhao et al. 2019). Due to optimization inconsistency between the main and auxiliary tasks, such approaches have limited benefits.

As we know, different depths represent distinct levels of abstraction in deep learning. Features with higher resolutions learned in shallow layers have fine spatial localization but lack semantics (Li and Chen 2020). Hence, we hypothesize that lower-level features are also important for discriminating foreground pixels. Hence, a Multi-level Auxiliator is designed for counting network to assist in refining coarse-to-fine features, see Figure 3 (bottom). Three levels of representations (F_l , F_m and F_h) with different resolutions are drawn from shallow, middle and high intermediate layers. Afterwards, low- and middle-level features are processed by max pooling and 1×1 convolution to be aligned with high-level feature maps. Then summation operation is used to integrate them. The fused features are fed into the sequence of 3×3 , 1×1 convolutions, and the *sigmoid* non-linear activation is utilized to generate the confidence map with background removed. The supervision signals from auxiliary task are backforward split into three routes to collaboratively optimize semantic-specific features.

We visually demonstrate our hypothesis in Figure 5, which shows that low-level features indeed focus on detailed localization, whereas high level encodes abstract semantics. Interestingly, middle-level representation yield higher response to background pixels. Thereby, the Multi-level Auxiliator is essential to our goal of driving features located at

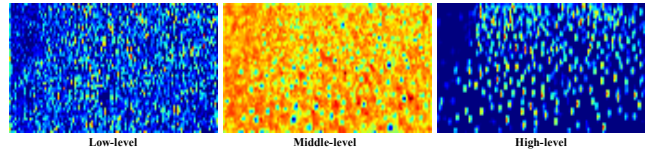


Figure 5: Visualization of features at low, middle and high levels. The Multi-level Auxiliator guides the low-level features to involve more details compared to high level with abstract density distribution embedded, whereas middle level concentrates on noisy background regions.

different depths to embed diverse cues of density distribution and background information.

Semi-Supervised Optimization. We attribute the poor handling of background noises to the latent imbalance of pixels occupied by background and people heads in crowd datasets. With a view to forcing the network to capture discriminative features for robustly perceiving complex noises, a semi-supervision strategy is incorporated to enlarge the background samples. As illustrated in Figure 3, a certain percentage rate (λ) of pure background images are stochastically inserted into the input batch. Through non-linear transformation of the backbone network, predicted density map, crowd confidence, and background maps are generated. Therefore, our holistic supervision L consists of three sub-terms: L_d and L_c for supervised density estimation and confidence prediction, and L_b for unsupervised background cognition. Then the overall optimization objective of our STNet is defined as:

$$L = L_d(W_d, I_c) + L_c(W_c, I_c) + L_b(W_c, I_b), \quad (6)$$

where I_c and I_b indicate the inputs of congested scenes and background images, whereas W_d and W_c denote the sets of weight matrices collected from core density estimation and side confidence prediction, respectively. The first term is calculated using conventional Euclidean distance between the predicted density map ($D_d(W_d, I_c)$) and density ground truth (D). Let N denote batch size, then

$$L_d(W_d, I_c) = \frac{1}{(1-\lambda)N} \sum_{i=1}^{(1-\lambda)N} \|D_d(W_d, I_{c,i}) - D_i\|_2^2 \quad (7)$$

The second term $L_c(W_c, I_c)$ in loss function (6) is for the Auxiliator, which is implemented utilizing binary cross entropy between the predicted confidence map ($\hat{D}_d(W_d, I_c)$) and crowd label map C . We have:

$$L_c(W_c, I_c) = \frac{1}{(1-\lambda)N} \sum_{i=1}^{(1-\lambda)N} \sum_{(p,q) \in I_{(c,i)}} (C_i^{p,q} \log \hat{D}_d(W_d, I_{c,i})^{p,q} + (1 - C_i^{p,q}) \log(1 - \hat{D}_d(W_d, I_{c,i})^{p,q})) \quad (8)$$

In order to combat the inconsistency of two optimization directions and consider global density level at the same time, we derive crowd label by binarizing from density map D in

terms of the average density values.

$$D_{p,q} = \begin{cases} 1 & \text{if } \hat{D}_{p,q} \geq 0.5 \times \text{Mean}(D) \\ 0 & \text{otherwise,} \end{cases} \quad (9)$$

where the purpose of $\text{Mean}(D)$ is to embed holistic density information of crowd images into auxiliary deep supervisions. The last term $L_b(W_c, I_b)$ is designed for noise-focusing optimization without additional labels on the basis of L_2 norm of predicted background $B(W_c, I_b)$.

$$L_b(W_c, I_b) = \frac{1}{\lambda N} \sum_{i=1}^{\lambda N} \|B(W_c, I_{b,i})\|_2^2 \quad (10)$$

To guarantee learning of two tasks with equal contribution and get rid of cumbersome weights tuning, all optimization terms are treated equally with the same weight of “1”.

Experiments

Experiment Setup

The first ten layers of a pretrained VGG-16 are leveraged to form the backbone in STNet, followed by six diversity enhancer modules with dense connections. Each scale tree has depth = 2 and degree = 3. Low-and middle-level supervisions are imposed on the fifth and top layers in backbone, respectively. During each epoch, we augment the input crowd samples by cropping fixed-size patches of 176×176 at random locations and then the image patches are randomly flipped horizontally and vertically. In addition, random color jitter is applied to enlarge the training set. Different from other models seeking for auxiliary tasks, the training pattern of our method is completely end-to-end. The Adam algorithm with initial learning rate of 0.0001 is used to optimize our model and the batch size is uniformly set to 16. The pure background samples for semi-supervision training procedure are 675 images without people involved, which are taken from Internet and are used for all 4 training datasets. After the training, the Multi-level Auxiliator is removed and the main stream of density estimation with strong representing ability is used to infer density maps. The proposed STNet is implemented in Pytorch (Paszke et al. 2017) and all experiments are carried out on a single Titan Xp GPU.

Comparisons with State-of-the-art

We first qualitatively compare the performance of the proposed STNet with recent prominent approaches (Jiang et al. 2019; Liu et al. 2019b; Ma et al. 2019; Bai et al. 2020; Liu, Yang, and Ding 2020) on four datasets. It is worth noting that some existing approaches profit from novel frameworks with conventional density map or new ground truths. Take BL (Ma et al. 2019) and ADSCNet (Bai et al. 2020) for example. They propose new types of ground truth to boost prediction accuracy. In this paper, we focus on investigating novel counting framework embracing higher representation capacity and all our results are acquired by training the model with original ground truth. It is more reasonable to compare with these frameworks where the loss is computed

on the given ground truth of original density map. Qualitative results are shown in Table 1.

On both datasets of ShanghaiTech Part_A and Part_B, our model surpasses all existing methods and achieves the state-of-the-art result with MAE 52.85 and 6.25, which are lower than that of the latest ADSCNet. It should be noted that the success of ADSCNet (55.4 & 6.4) (CVPR20) is mainly attributed to ground truth correction operation. When compared with its counterpart ADNet (61.3 & 7.6) trained using plain density map, our model obtains greater improvements: 13.8% and 17.8% lower for Part_A and Part_B accordingly, which illustrates that our method has more powerful ability of representation learning in the case of either dense or sparse crowd datasets. As for UCF-QNRF dataset, our method achieves the third-best result compared with all existing methods and the second-best result of MAE 87.88 among the set of approaches that use the original ground truth, which is only 1.5% higher than that of AMRNet (ECCV20). Note that AMRNet only gains slightly better performance on this dataset and reports relatively weak results on ShanghaiTech Part_A and Part_B. Benefiting from ground truth correction, ADSCNet obtains the best result on UCF-QNRF. For fair comparison, here we emphasize the comparison with its primary version ADNet. It can be observed that our STNet performs better (MAE 87.88) than ADNet (MAE 90.1), which demonstrates that our algorithm is able to excel in capturing informative features. Finally, on the tiny UCF_CC_50, our method also achieves the best result with an MAE of 161.96, which is 7.4% lower than that of the second-best approach ASNet (CVPR20).

Ablation Study

In this section, we conduct detailed ablation study on ShanghaiTech Part_A to demonstrate the effectiveness of components in the proposed STNet.

Effect of Scale Tree Diversity Enhancer. To investigate the effects of the Diversity Enhancer, we compare two networks: traditional CSRNet (Li, Zhang, and Chen 2018) and CSRNet+. CSRNet+ means the STNet without tree enhancer, which is implemented by replacing the enhancers in STNet with traditional CSRNet units. The quantitative results in Table 2 show that the proposed Diversity Enhancer is remarkably better than the widely-used layer-wise dilated convolution in CSRNet, while introducing fewer parameters at the same time. The improvement is mainly attributed to the fact that the scale tree provides huger diversity of scales.

Effect of Multi-level Auxiliator. To evaluate the merit of Deep Auxiliator, we compare several variants of CSRNet and STNet. As shown in Table 3, CSRNet+ with Multi-level Auxiliator achieves 5.9% higher MAE than that without the designed auxiliator. In order to further investigate the impacts of features extracted from different levels, we evaluate four variants of STNet: from STNet without auxiliator to STNet with auxiliator using high-middle-low-level. The quantitative MAE values demonstrate that all three levels of the auxiliator contribute to the final performance. Especially, missing low-level information brings more dramatic decreases in MAE. This phenomenon further supports the observation that low-level features encode abundant de-

Methods	Part_A		Part_B		UCF-QNRF		UCF_CC_50	
	MAE	MSE	MAE	MSE	MAE	MSE	MAE	MSE
TEDNet(CVPR19)	64.2	109.1	8.2	12.8	113	188	249.4	354.5
ADCrowdNet (CVPR19)	63.2	98.9	7.6	13.9	-	-	257.1	363.5
PACNN + CSRNet (CVPR19)	62.4	102.0	7.6	11.8	-	-	241.7	320.7
CANet (CVPR19)	62.3	100.0	7.8	12.2	107	183	212.2	243.7
SPN+L2SM (ICCV19)	64.2	98.4	7.2	11.1	104.7	173.6	188.4	315.3
MBTTBF-SCFB (ICCV19)	60.2	94.1	8.0	15.5	97.5	165.2	233.1	300.9
DSSINet (ICCV19)	60.63	96.04	6.85	10.34	99.1	159.2	216.9	302.4
S-DCNet (ICCV19)	58.3	95.0	6.7	10.7	104.4	176.1	204.2	301.3
ASNet (CVPR20)	57.78	90.13	-	-	91.59	159.71	174.84	251.63
ADNet (CVPR20)	61.3	103.9	7.6	12.1	90.1	147.1	245.4	327.3
AMRNet (ECCV20)	61.59	98.36	7.02	11.00	86.6	152.2	184.0	265.8
AMSNet (ECCV20)	58.0	96.2	7.1	10.4	103	165	208.6	296.3
BL (ICCV19)	62.8	101.8	7.7	12.7	88.7	154.8	229.3	308.2
ADSCNet (CVPR20)	55.4	97.7	6.4	11.3	71.3	132.5	198.4	267.3
STNet (proposed)	52.85	83.64	6.25	10.30	87.88	166.44	161.96	230.39

Table 1: Comparison with state-of-the-art methods on ShanghaiTech (Part_A and Part_B), UCF-QNRF and UCF_CC_50 datasets. Best results are shown in boldface.

	CSRNet	CSRNet+(w/o Enhancer)	STNet
Params.	16.26M	25.10M	15.56M
MAE	68.2	58.7	52.8
MSE	115.0	97.2	83.6

Table 2: The impacts of Scale Tree Diversity Enhancer on ShanghaiTech Part_A dataset.

tailed localization information, which is in favor of purifying crowd features. To combat the inconsistency of two optimization directions (density estimation & crowd confidence) and take the holistic density distribution into account, we disentangle ground truth of crowd label from density map according to Equ. 9. To illustrate the effectiveness of this generation strategy, we compare it with the approach in the recent work (Zhao et al. 2019) with binaryzation threshold value of 0 and our algorithm brings 14.19% lower in MAE (61.59% \rightarrow 52.85%).

	MAE	MSE
CSRNet+ w/o Auxiliator	62.378	100.951
CSRNet+ w/ Auxiliator	58.711	97.197
STNet w/ BT=0	61.591	100.313
STNet w/o Auxiliator	59.296	98.699
STNet w/ H.A	57.66	98.93
STNet w/ H.M.A	57.519	98.86
STNet w/ H.M.L.A	52.85	83.64

Table 3: Multi-level Auxiliator ablation study on ShanghaiTech Part.A. H.A, H.M.A and H.M.L.A indicates the auxiliator uses high-level only, high and middle-level only, and all three levels, respectively.

Effect of Semi Supervision with Pure Background Sam-

ples. Table 4 shows quantitative comparisons between the STNet with and without using pure background images for training the Multi-level Auxiliator. It is observed that additional background samples effectively boost the capacity of capturing representations encoding background information, thereby leading to precise recognition of pixels occupied by people.

	w/o Semi Supervision		w/ Semi Supervision	
	MAE	MSE	MAE	MSE
Part_A	56.47	97.19	52.85	83.64
Part_B	6.71	11.36	6.25	10.30
QNRF	89.81	168.29	87.88	166.44

Table 4: Semi Supervision ablation of our STNet on ShanghaiTech Part_A, Part_B and UCF_QNRF datasets.

Conclusion

In this paper, we present a novel network, STNet, which consistently addresses the challenges of drastic scale variations, density changes, and complex background. The issues of scale variations are alleviated using a novel tree-based scale enhancer, whereas a Multi-level Auxiliator is designed to accurately filter out pixels from complex background and adapt to density changes. Extensive experiments on four popular crowd counting datasets demonstrate the superiority of our STNet over the state-of-the-art approaches, while employing fewer parameters at the same time. A simple yet effective idea of using pure background images to deal with crowd and background sample imbalance problem is also introduced. This idea can be easily incorporated in other crowd counting algorithms for further accuracy improvement. For future work, we will investigate possibility of using self-supervision and more unlabelled scenes to improve crowd counting performance.

References

- Bai, S.; He, Z.; Qiao, Y.; Hu, H.; Wu, W.; and Yan, J. 2020. Adaptive Dilated Network With Self-Correction Supervision for Counting. In *Proceedings of the IEEE/CVF Conference on Computer Vision and Pattern Recognition*, 4594–4603.
- Cao, X.; Wang, Z.; Zhao, Y.; and Su, F. 2018. Scale aggregation network for accurate and efficient crowd counting. In *Proceedings of the European Conference on Computer Vision (ECCV)*, 734–750.
- Chan, A. B.; Liang, Z.-S. J.; and Vasconcelos, N. 2008. Privacy preserving crowd monitoring: Counting people without people models or tracking. In *2008 IEEE Conference on Computer Vision and Pattern Recognition*, 1–7. IEEE.
- Chen, K.; Gong, S.; Xiang, T.; and Change Loy, C. 2013. Cumulative attribute space for age and crowd density estimation. In *Proceedings of the IEEE conference on computer vision and pattern recognition*, 2467–2474.
- Chen, K.; Loy, C. C.; Gong, S.; and Xiang, T. 2012. Feature mining for localised crowd counting. In *BMVC*, volume 1, 3.
- Gao, B.-B.; Xing, C.; Xie, C.-W.; Wu, J.; and Geng, X. 2017. Deep label distribution learning with label ambiguity. *IEEE Transactions on Image Processing* 26(6): 2825–2838.
- Idrees, H.; Saleemi, I.; Seibert, C.; and Shah, M. 2013. Multi-source multi-scale counting in extremely dense crowd images. In *Proceedings of the IEEE conference on computer vision and pattern recognition*, 2547–2554.
- Idrees, H.; Tayyab, M.; Athrey, K.; Zhang, D.; Al-Maadeed, S.; Rajpoot, N.; and Shah, M. 2018. Composition loss for counting, density map estimation and localization in dense crowds. In *Proceedings of the European Conference on Computer Vision (ECCV)*, 532–546.
- Jiang, X.; Xiao, Z.; Zhang, B.; Zhen, X.; Cao, X.; Doermann, D.; and Shao, L. 2019. Crowd counting and density estimation by trellis encoder-decoder networks. In *Proceedings of the IEEE Conference on Computer Vision and Pattern Recognition*, 6133–6142.
- Jiang, X.; Zhang, L.; Xu, M.; Zhang, T.; Lv, P.; Zhou, B.; Yang, X.; and Pang, Y. 2020a. Attention Scaling for Crowd Counting. In *Proceedings of the IEEE/CVF Conference on Computer Vision and Pattern Recognition*, 4706–4715.
- Jiang, X.; Zhang, L.; Zhang, T.; Lv, P.; Zhou, B.; Pang, Y.; Xu, M.; and Xu, C. 2020b. Density-Aware Multi-Task Learning for Crowd Counting. *IEEE Transactions on Multimedia*.
- Lempitsky, V.; and Zisserman, A. 2010. Learning to count objects in images. In *Advances in neural information processing systems*, 1324–1332.
- Li, D.; and Chen, Q. 2020. Dynamic Hierarchical Mimicking Towards Consistent Optimization Objectives. In *Proceedings of the IEEE/CVF Conference on Computer Vision and Pattern Recognition*, 7642–7651.
- Li, M.; Zhang, Z.; Huang, K.; and Tan, T. 2008. Estimating the number of people in crowded scenes by MID based foreground segmentation and head-shoulder detection. In *2008 19th International Conference on Pattern Recognition*, 1–4.
- Li, Y.; Zhang, X.; and Chen, D. 2018. Csrnet: Dilated convolutional neural networks for understanding the highly congested scenes. In *Proceedings of the IEEE conference on computer vision and pattern recognition*, 1091–1100.
- Liu, L.; Qiu, Z.; Li, G.; Liu, S.; Ouyang, W.; and Lin, L. 2019a. Crowd counting with deep structured scale integration network. In *Proceedings of the IEEE International Conference on Computer Vision*, 1774–1783.
- Liu, N.; Long, Y.; Zou, C.; Niu, Q.; Pan, L.; and Wu, H. 2019b. Adcrowdnet: An attention-injective deformable convolutional network for crowd understanding. In *Proceedings of the IEEE Conference on Computer Vision and Pattern Recognition*, 3225–3234.
- Liu, S.; Johns, E.; and Davison, A. J. 2019. End-to-end multi-task learning with attention. In *Proceedings of the IEEE Conference on Computer Vision and Pattern Recognition*, 1871–1880.
- Liu, W.; Salzmann, M.; and Fua, P. 2019. Context-aware crowd counting. In *Proceedings of the IEEE Conference on Computer Vision and Pattern Recognition*, 5099–5108.
- Liu, X.; Yang, J.; and Ding, W. 2020. Adaptive Mixture Regression Network with Local Counting Map for Crowd Counting. *arXiv preprint arXiv:2005.05776*.
- Ma, Z.; Wei, X.; Hong, X.; and Gong, Y. 2019. Bayesian loss for crowd count estimation with point supervision. In *Proceedings of the IEEE International Conference on Computer Vision*, 6142–6151.
- Miao, Y.; Lin, Z.; Ding, G.; and Han, J. 2020. Shallow Feature Based Dense Attention Network for Crowd Counting. In *AAAI*, 11765–11772.
- Onoro-Rubio, D.; and López-Sastre, R. J. 2016. Towards perspective-free object counting with deep learning. In *European Conference on Computer Vision*, 615–629. Springer.
- Paszke, A.; Gross, S.; Chintala, S.; Chanan, G.; Yang, E.; DeVito, Z.; Lin, Z.; Desmaison, A.; Antiga, L.; and Lerer, A. 2017. Automatic differentiation in pytorch.
- Pham, V.-Q.; Kozakaya, T.; Yamaguchi, O.; and Okada, R. 2015. Count forest: Co-voting uncertain number of targets using random forest for crowd density estimation. In *Proceedings of the IEEE International Conference on Computer Vision*, 3253–3261.
- Sam, D. B.; Surya, S.; and Babu, R. V. 2017. Switching convolutional neural network for crowd counting. In *2017 IEEE Conference on Computer Vision and Pattern Recognition (CVPR)*, 4031–4039. IEEE.
- Shen, Y.; Tan, S.; Sordoni, A.; and Courville, A. 2019. Ordered neurons: Integrating tree structures into recurrent neural networks. In *Proceedings of ICLR*.
- Sidla, O.; Lypetsky, Y.; Brandle, N.; and Seer, S. 2006. Pedestrian detection and tracking for counting applications

in crowded situations. In *2006 IEEE International Conference on Video and Signal Based Surveillance*, 70–70. IEEE.

Simonyan, K.; and Zisserman, A. 2014. Very deep convolutional networks for large-scale image recognition. *arXiv preprint arXiv:1409.1556* .

Sindagi, V. A.; and Patel, V. M. 2017. Generating high-quality crowd density maps using contextual pyramid cnns. In *Proceedings of the IEEE International Conference on Computer Vision*, 1861–1870.

Sindagi, V. A.; and Patel, V. M. 2019. Multi-level bottom-top and top-bottom feature fusion for crowd counting. In *Proceedings of the IEEE International Conference on Computer Vision*, 1002–1012.

Subburaman, V. B.; Descamps, A.; and Carincotte, C. 2012. Counting people in the crowd using a generic head detector. In *2012 IEEE Ninth International Conference on Advanced Video and Signal-Based Surveillance*, 470–475. IEEE.

Xiong, H.; Lu, H.; Liu, C.; Liu, L.; Cao, Z.; and Shen, C. 2019. From open set to closed set: Counting objects by spatial divide-and-conquer. In *Proceedings of the IEEE International Conference on Computer Vision*, 8362–8371.

Zhang, Y.; Zhou, D.; Chen, S.; Gao, S.; and Ma, Y. 2016. Single-image crowd counting via multi-column convolutional neural network. In *Proceedings of the IEEE conference on computer vision and pattern recognition*, 589–597.

Zhao, M.; Zhang, J.; Zhang, C.; and Zhang, W. 2019. Leveraging heterogeneous auxiliary tasks to assist crowd counting. In *Proceedings of the IEEE Conference on Computer Vision and Pattern Recognition*, 12736–12745.

Zhao, T.; and Nevatia, R. 2003. Bayesian human segmentation in crowded situations. In *2003 IEEE Computer Society Conference on Computer Vision and Pattern Recognition, 2003. Proceedings.*, volume 2, II–459. IEEE.